

Supplementary Materials:

ADDG : An Adaptive Domain Generalization Framework for Prostate Cross-Plane MRI Segmentation

Anonymous Authors

1 DETAILED ARCHITECTURE OF MDOS-NET

1.1 2D + 3D Mix Encoder and Decoder in 2.5D Multi-Path Segmentation Network

The architecture of the 2D + 3D Mix Encoder and Decoder in the 2.5D Multi-Path Segmentation Network of MDOS-Net is shown in Figure 1 and Figure 2, which is a supplementary figure for section 3.2.1 in the paper.

1.2 Organ-Specific Mesh Template

A Comparison of the ellipsoidal mesh template and organ-specific mesh template is shown in Figure 3, as a supplementary figure for section 3.2.3 in the paper.

2 EXPERIMENTAL DATA DETAILS

As presented in Table 1, we can find that almost the whole dataset for prostate gland segmentation are scanned from axial view, and even in some datasets (i.e. PROMISE12) of the training data split, the axial plane T2w MRI were collected from heterogeneous institutions, which has the different field strength, coil setting, and manufacturers.

3 RESULTS VISUALIZATION

We provide more visualization results on sagittal plane MRI testing data and coronal plane MRI testing data respectively. First, the overall performance of voxel-based image segmentation methods (i.e., MNet, nnUNet) does not perform as well as mesh deformation-based methods (i.e., ADDG, Voxel2Mesh, and Vox2Cortex). Second, compared to Voxel2Mesh as well as Vox2Cortex, our method is able to produce tighter boundary predictions (significantly less False Positive and False Negative areas) on most slices, with fewer prediction errors in the more difficult segmentation of samples (e.g., Figure 5, row 1 and row 2, and Figure 6, row 6) area (fewer False Positive regions).

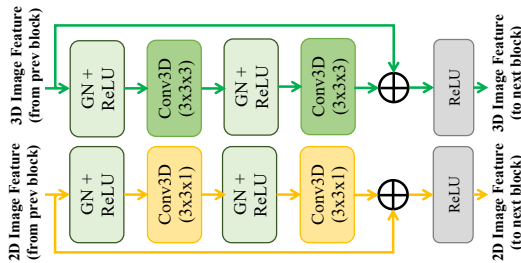


Figure 1: Detail of 2D + 3D Encoder Block (2D + 3D Mix Conv Block)

2024-04-20 11:22. Page 1 of 1-3.

4 ILLUSTRATION OF SINGLE- AND MULTI-PLANAR PROSTATE T2W MRI

As shown in Figure 4, for better understanding the anisotropic and multi-planar imaging properties of prostate T2w MRIs, we visualized one sample from each dataset in the training and testing domains: in the “Testing domains”, the diagonal line shows the scans in three planes (sagittal plane MRI scan is marked by orange box, and coronal plane MRI scan is marked by red box) from a ProstateX-Seg-Hi-Res case, and each row represents a particular plane scan and its multi-plane reconstruction (MPR) results in other planes. Each row represents a scan in one plane and its multi-plane reconstruction in the other planes, and we can see that scans in one plane have significant Gaussian blurring when observed in the other planes; in “Training domains”, we can see scans from

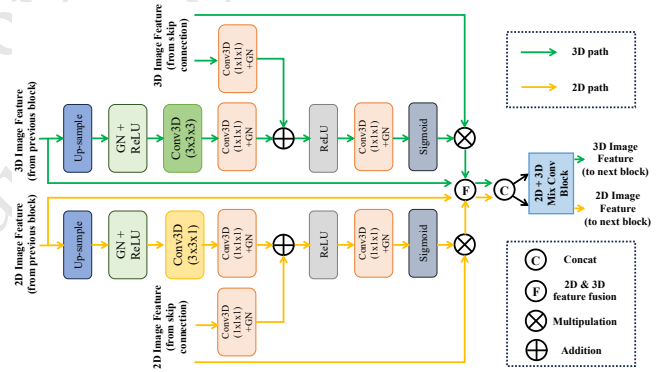


Figure 2: Detail of 2D + 3D Decoder Block (2D + 3D Mix Dec Block)

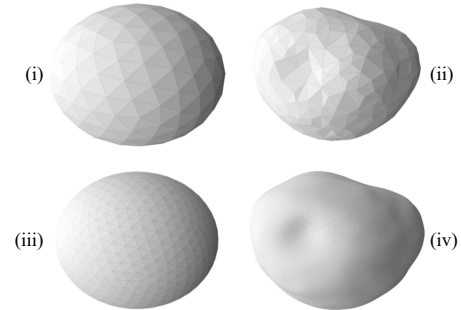


Figure 3: i) Ellipsoidal mesh template, with 162 vertices and 324 faces; ii) Prostate mesh template, with 388 vertices and 762 faces; iii) Ellipsoidal mesh template, with 642 vertices and 1284 faces; and iv) Prostate mesh template, with 51268 vertices and 102532 faces.

Table 1. Experimental Data Details.

Split	Dataset	Scan	Subset (Institution)	Case num	Field strength (T)	Resolution(in/ through plane) ([mm])	Endorectal Coil	Manufactor
Testing	ProstateX-Seg-Hi-Res	sagittal	-	66	3	0.56/[3 – 4]	No	Siemens
		coronal	-	66	3	[0.56 – 0.6]/[3 – 4.5]	No	Siemens
	MSD-Prostate	axial	-	32	3	[0.6 – 0.625]/[3.6 – 4]	Surface	Siemens
Training / Validation	PROMISE12	axial	UCL	18	1.5 and 3	[0.325 – 0.625]/[3 – 3.6]	No	Siemens
			BIDMC	16	3	0.25/[2.2 – 3]	Endorectal	GE
			HK	16	1.5	0.625/3.6	Endorectal	Siemens
	I2CVB	axial	-	19	3	[0.67 – 0.79]/1.25	No	Siemens
	NCI-ISBI13	axial	BMC	30	1.5	0.4/3	Endorectal	Phlips
			RUNMC	30	3	[0.6 – 0.625]/[3.6 – 4]	Surface	Siemens

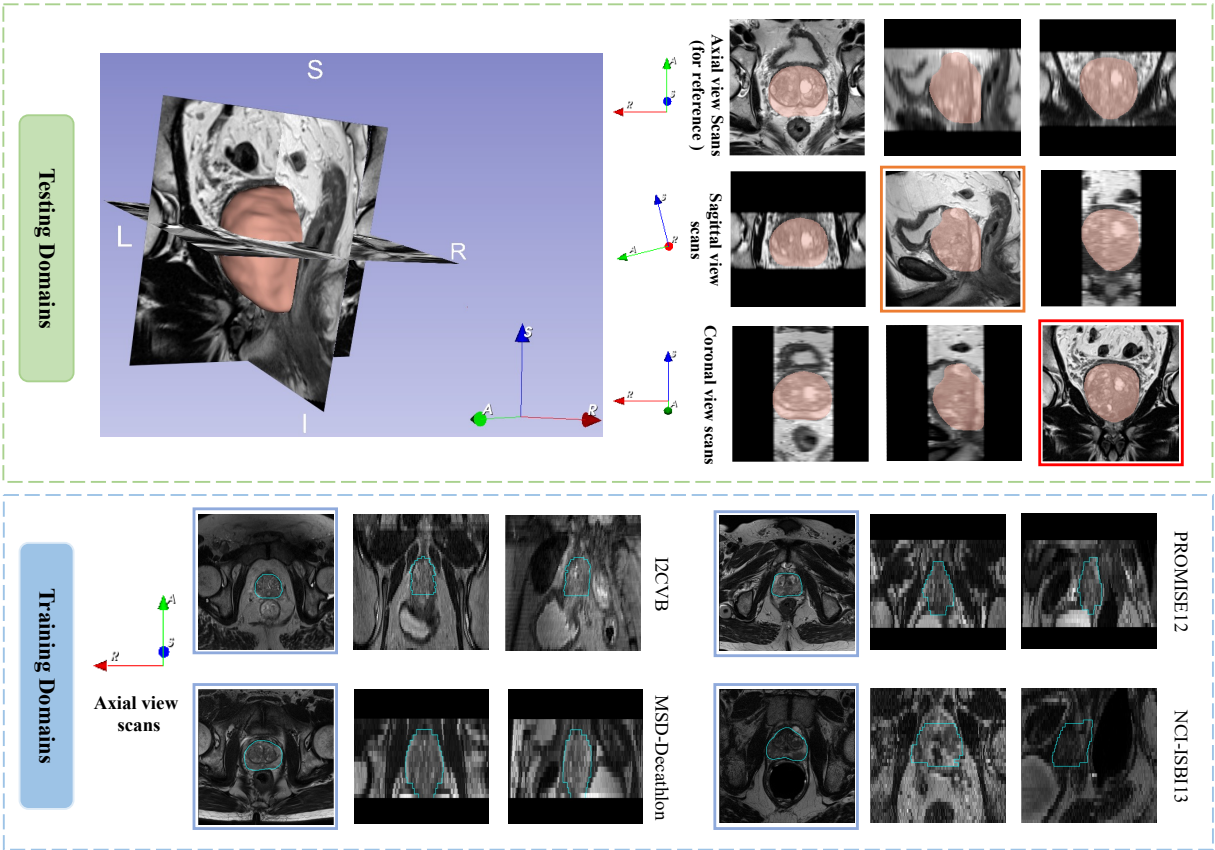


Figure 4: Illustration of Single- and Multi-Planar Prostate T2w MRI

the four datasets (PROMISE12, MSD-Decathlon, I2CVB, and NCI-ISBI13): similarly, each of the three 2D MRI slices represents an axial plane MRI scan (marked by the blue box) and its MPR in the other planes. We can see the difference in resolution of the MRI scans in the axial plane caused by the difference in inter-plane resolution when observed in the other planes, and we can find that even I2CVB, which has the highest inter-plane resolution, has obvious jagged artifacts in its annotation when observed in the coronal and sagittal planes, and its images still show a certain degree of

Gaussian blurring, which we believe that this somehow explains the significant performance degradation of voxel-based segmentation methods when segmenting on unseen planes MRI scans, as such methods are highly dependent on the resolution of the image, and the axial plane MRI data makes the image itself unclear due to its anisotropy, which also makes the manual annotation in the axial plane while observing in the coronal and sagittal planes are not accurate.

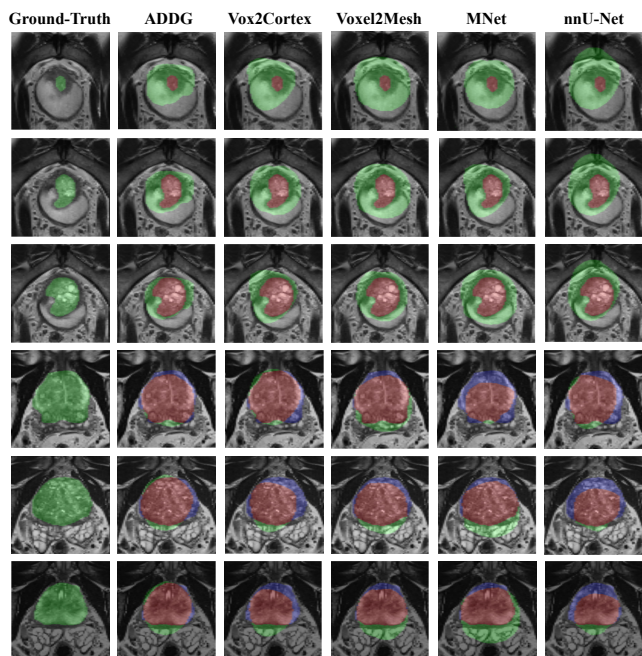


Figure 5: Visualization on the coronal plane MRI data, where red mask denotes true positive, green mask in columns 1-5 denotes false positive, and purple mask denotes false negative.

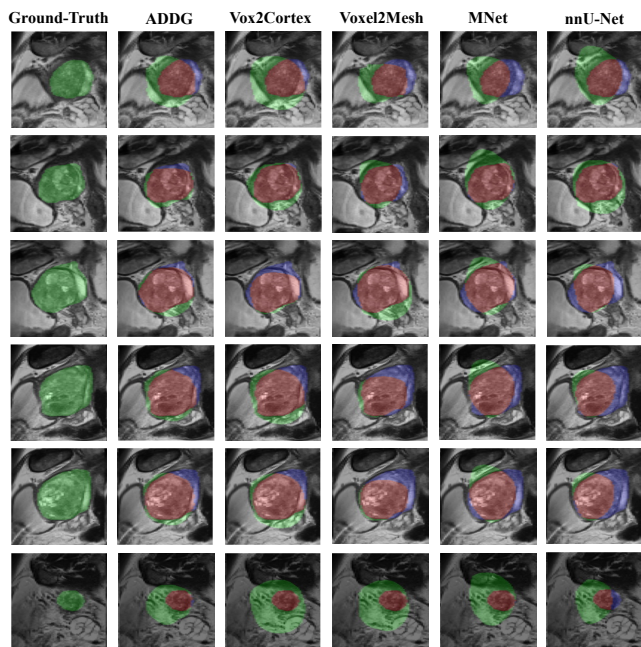


Figure 6: Visualization on the sagittal plane MRI data, where red mask denotes true positive, green mask in columns 1-5 denotes false positive, and purple mask denotes false negative.